Dynamic Properties of High-Purity Beryllium

D. R. CHRISTMAN* AND N. H. FROULA†
General Motors Corporation, Warren, Mich.

Tests were conducted on high-purity beryllium plate to determine the Hugoniot equation of state and shock wave profile up to 50 kbar, and the spall threshold for elastic pulse widths of 0.2, 0.4, and 0.8 μsec, using flat-plate impact techniques. Tests were carried out at material temperatures of 22°C and 260°C. This beryllium was found to have a two-wave elastic-plastic structure with a highly ramped transition from the elastic precursor to the plastic wave. No change in the material equation of state was observed for a temperature increase of 22°C to 260°C. The spall threshold (as defined by the onset of microcracking) was found to be time dependent, with impact velocity required for spall increasing with decreasing pulse width, and temperature dependent, with velocity increasing with increasing temperature.

Introduction

ANALYSIS of the response of materials and structures to impulsive loads requires detailed knowledge of dynamic material behavior, including stress wave propagation characteristics. Impulsive loading might arise from several causes: 1) weapons effects; 2) high-velocity impact; or 3) high-energy rate forming. Numerous reviews of material behavior under dynamic loading conditions, including discussion of laboratory experimental techniques have appeared in the literature.[1] This paper presents some results from a comprehensive study of the dynamic properties of wrought, polycrystalline beryllium plate of relatively high purity. Complete results of the study are given in Ref. 2.

Among the material dynamic properties that can be measured in the laboratory are the Hugoniot equation of state (EOS), which defines material behavior under shock loading, and the spall threshold, which defines the dynamic tensile fracture behavior. Measurement of these properties under controlled laboratory conditions provides experimental inputs to the development of analytical models of material behavior. These models are used in computer codes for the prediction and assessment of material response to impulsive loads.

Hugoniot EOS

In determining the Hugoniot equation of state and shock wave profile, flat-plate impact is used to generate a plane shock wave. A planar wave results in a one-dimensional condition of uniaxial strain (i.e., zero lateral strain) which greatly simplifies the measurement and analysis of material behavior. Measurements are made of wave velocity, stress, and/or mass velocity in the direction of shock wave propagation. From a given experiment where at least two of these parameters are measured, and from the Rankine-Hugoniot conditions for conservation of momentum and mass across an elastic-plastic shock (see Fig. 1),

$$P = P_{HEL} + \rho_1(U_s - u_e)(u_p - u_e) \quad (1)$$

$$\rho_0/\rho_2 = (1 - u_e/C_L)[1 - (u_p - u_e)/(U_s - u_e)] \quad (2)$$

where $P_{HEL} = \rho_0 C_L u_e$, P is stress, ρ is density, C_L and U_s are elastic and plastic wave velocity, and u_e and u_p are elastic and plastic particle velocities, an equation-of-state point can be calculated. A series of these points defines the locus of final states reached across the shock front and is called the Hugoniot. This locus is usually presented in the $P - u_p$, $U_s - u_p$, or $P - v$ planes (v = specific volume).

Spall Threshold

Spallation may be defined as fracture of a material upon being subjected to a tensile stress resulting from the interaction of rarefaction waves. Specifically, for this work the incipient spall threshold was defined as the minimum impact velocity for a given pulse width that caused material fracture. The incipient fractures were found by sectioning, polishing, and etching the shock-loaded specimen and examining at 60× magnification.

For the elastic-plastic wave structure existing in beryllium at stresses near the spall threshold, it is difficult to define the tensile pulse width at the spall plane due to the complex wave interactions in the material. To illustrate, consider the idealized situation for an elastic-perfectly plastic material, as shown in the simplified x-t diagram in Fig. 2 (drawn as if no fracture occurs and with some wave interactions omitted for clarity). The elastic pulse width is given by

$$\Delta T_e = T_2 - T_0 = 2h_p/C_L \quad (3)$$

and the plastic pulse width by

$$\Delta T_p = T_3 - T_1 = 2h_p/U_s \quad (4)$$

assuming $h_t = 2h_p$ (where h_t and h_p are target and impactor thickness, respectively) and compressive wave velocity equals rarefaction wave velocity. In addition, total pulse width ($T_t - T_0$) or peak pulse width ($T_2 - T_1$) could also be considered.[3] Since the exact mechanisms of fracture due to such a wave system are, at present, poorly understood, and may require consideration of stress rate and stress gradient as well as pulse width,[4,5] it is not possible to precisely define the spall-producing conditions. Therefore, the elastic

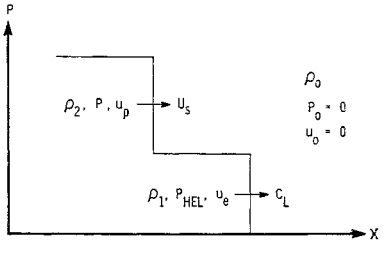

Fig. 1 Elastic-plastic wave.

Presented as Paper 69-360 at the AIAA Hypervelocity Impact Conference, Cincinnati, Ohio, April 30–May 2, 1969; submitted May 5, 1969; revision received September 4, 1969. This research was supported in part by Sandia Corporation under Contract 16-5741.

* Section Engineer, Materials and Structures Laboratory, Manufacturing Development.

† Research Physicist; presently Staff Physicist, Systems, Science and Software, La Jolla, Calif.

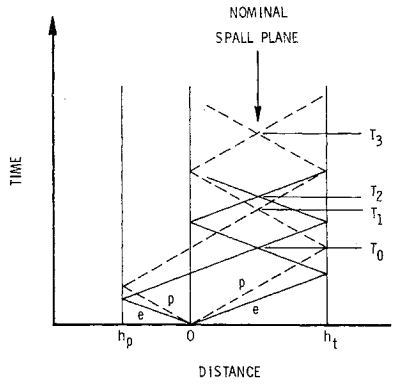

Fig. 2 Elastic-plastic wave positions, like materials.

approximation given in Eq. (3) is used in this paper for the nominal pulse width, since it permits direct comparison with other beryllium spall studies.[6,7]

Experimental Techniques

Hugoniot EOS and wave profile measurements were made using flat-plate impact techniques.[8] Measurements of stress, wave velocity, and/or particle velocity were made using x-cut quartz crystals,[9] slanted resistance wires,[10] and a laser velocity interferometer.[11] Measurements at 260°C were made with quartz crystals only.

Spall threshold tests were made using flat-plate impact techniques in which the target thickness was maintained at twice the impactor thickness (putting the nominal spall plane at the center of the target). The targets utilized a tapered (6°) plug inserted into an annular ring of the same material to minimize the effects of edge rarefactions.[12]

All tests were performed with compressed-gas guns of either 63.5-mm or 102-mm bore. The guns were equipped with systems to measure projectile velocity and impact tilt, as well as diagnostic equipment for data recording. Special heating equipment was designed and built for the elevated temperature tests. For elevated temperature tests, heat-up time and time-at-temperature before test were nominally 10 min each. The experimental techniques are described in detail in Ref. 2.

Results

Material Properties

The beryllium used for all tests was supplied in the form of 12.7-mm ($\frac{1}{2}$-in.) plate by the Dow Chemical Company, Rocky Flats Division. The beryllium content (by weight) was 99.4% and the beryllium oxide content was 0.03%. The plate was prepared by high-temperature rolling of vacuum-induction cast scrap material.[13,14] The material was relatively coarse-grained (approximately ASTM 2, average grain size $\simeq$ 0.2 mm) and equiaxed with little evidence of texturing or fibering due to the plate rolling operation, as shown in Fig. 3. The material density was 1.845 ± 0.005 g/cc. Ultrasonics measurements gave 12.8 ± 0.2 mm/μsec for the longitudinal wave velocity C_L, and 8.8 ± 0.2 mm/μsec for the shear wave velocity C_s.

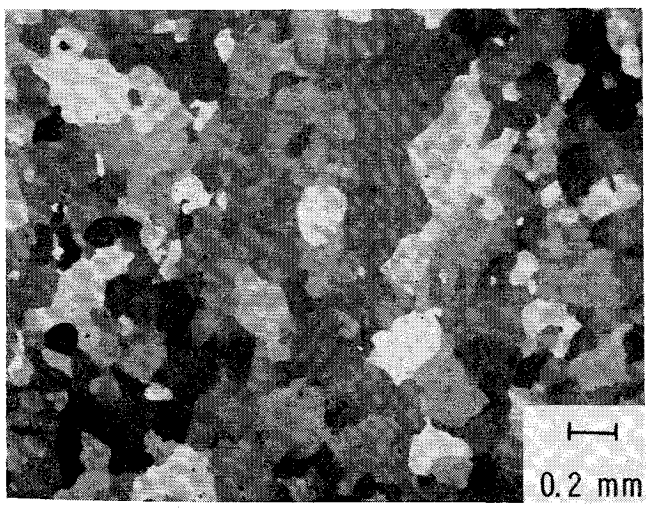

Fig. 3 Beryllium, as-received material (unetched).

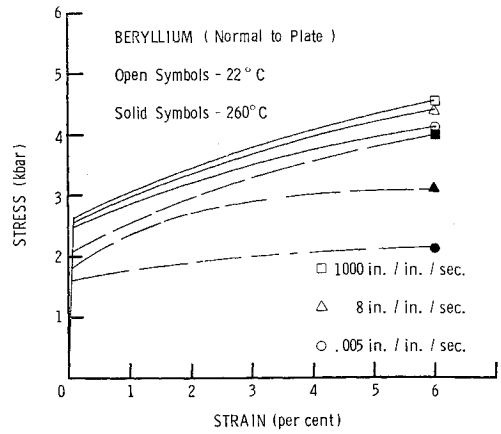

Fig. 4 Compressive stress-strain-strain rate behavior.

Uniaxial-stress compression tests were conducted at 22°C and 260°C, at strain rates up to 1000/sec. Results are given in Fig. 4. The material was slightly rate sensitive at 22°C (6% increase in yield stress) and significantly rate sensitive at 260°C (28% increase in yield stress), for a rate increase of almost six orders of magnitude. The plate showed anisotropic behavior, having approximately 17% higher yield in the direction normal to the plane of the plate as compared to parallel. All Hugoniot EOS and spall tests were conducted with the direction of wave propagation normal to the plane.

Hugoniot EOS

Hugoniot equation-of-state data obtained for beryllium at 22°C and 260°C are given in Fig. 5, in the $P - u_p$ plane. A second-order fit to the 22°C data gives

$$P = 0.8 + 149u_p + 32u_p^2 \qquad (5)$$

for $P > 3$ kbar;‡ u_p in mm/μsec. There is reasonable agree-

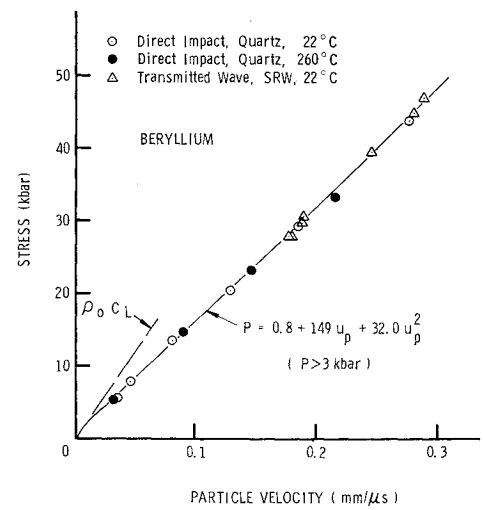

Fig. 5 Stress-particle velocity.

‡ kbar = 10^9 dyn/cm^2 = 14.5×10^3 psi.

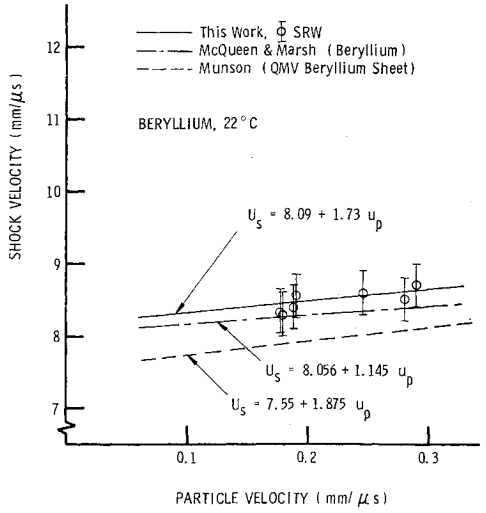

Fig. 6 Shock velocity-particle velocity.

ment (within experimental accuracy) between the room temperature fit and the 260°C data, indicating that the Hugoniot of this beryllium is temperature insensitive below 50 kbar for the temperature range of 22°C to 260°C. Below about 3 kbar, the Hugoniot curves downward (i.e., increasing slope with decreasing stress) and becomes tangent to the "elastic" Hugoniot, $\rho_0 C_L$ = 236 kbar/mm/μsec, at about one kbar.

When translated to the $U_s - u_p$ plane, the $P - u_p$ fit [(Eq. 5)] gives, approximately,

$$U_s = 8.09 + 1.73u_p \qquad (6)$$

which is shown in Fig. 6 with measured values of shock velocity from the slanted resistance wire (SRW) tests. Because of the ramped nature of the shock front, a unique value of the shock velocity could not be measured. The bars represent the spread in the arrival of the plastic wave, the circles indicate the point at which the amplitude of the plastic wave reached approximately 50% of its final value. Also shown in Fig. 6 are $U_s - u_p$ fits obtained by McQueen and Marsh[15] (150 < P < 1000 kbar) and by Munson[16] (P < 37 kbar) for different berylliums. Exact agreement of the results is not necessarily expected because of differences in stress range studied or material structure and composition.

Transmitted wave profile measurements did not show a sharp two-wave structure but rather a highly ramped transition from a poorly defined precursor of about 2 kbar to the plastic wave. Wave profiles for several values of target thickness and peak stress are given in Fig. 7. There was no significant difference in the precursor for target thicknesses of 6.3 and 11 mm, or for an increase in peak stress from 8 kbar to 18 kbar. The large increase in rise time in the plastic wave for an increase in propagation distance of 6.3 mm to 11 mm shows that a steady plastic wave profile has not developed at 8 kbar. The plastic wave rise time decreases with increasing impact velocity (peak stress), corresponding to an increase in plastic strain rate. A wave profile measured with the velocity interferometer is shown in Fig. 8. This record shows that a well-defined yield in uniaxial strain is not developed in polycrystalline beryllium under these impact conditions.

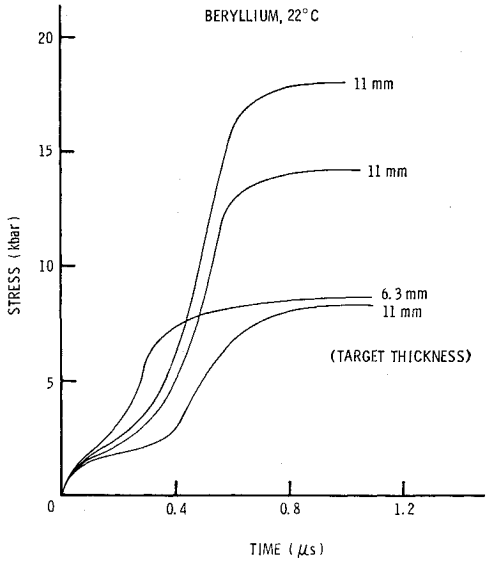

Fig. 7 Transmitted wave profiles, quartz.

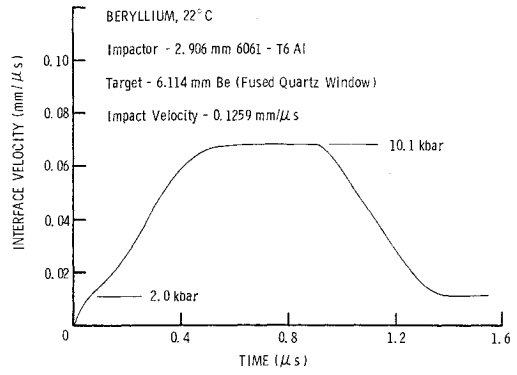

Fig. 8 Transmitted wave profile, velocity interferometer.

Qualitatively similar wave profiles were reported by Taylor[17] for polycrystalline beryllium at room temperature, using a free-surface capacitor technique, and by Froula[18] for polycrystalline S-200 beryllium at room and elevated temperatures, using quartz crystal techniques. Taylor also reported wave profiles for single crystal beryllium and noted that the initial yield was much sharper and that the precursor magnitude P_{HEL} could differ by more than a factor of 10 (approximately 4 to 40 kbar), depending on crystal orientation. This pronounced anisotropy may cause dispersion or smearing of the wave front in a polycrystalline material with randomly oriented grains.

For all SRW tests with beryllium impactors and targets, the final free surface velocity was found to be about 9% to 12% less than the impact velocity, as shown in Fig. 9. Symmetric impact (like materials) should give a final free surface velocity equal to the impact velocity, assuming no loss mechanisms are acting on the shock wave and free surface velocity equals twice particle velocity. The assumption that free surface velocity equals twice the particle velocity implies that the unloading path in the material is the same as the loading path. Differences could result in lower free surface velocity. Taylor[17] found similar behavior in copper, in a more extensive series of tests, and showed u_{fs}/V_I to be

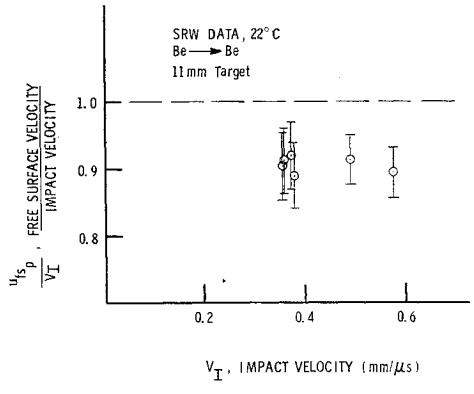

Fig. 9 Free surface data, slanted resistance wire (SRW).

Table 1 Beryllium spall results

Target thickness[a] h_t, mm	Target temp., °C	Spall threshold velocity V_s, mm/μsec	Pulse width, μsec: Elastic, ΔT_e	Plastic ΔT_p	Calc.[b] ΔT_c	Stress, kbar: Impact P_I	Calc.[b] P_s
2.54	22	0.061	0.20	0.31	0.29	5.4	3.3
2.54	260	0.087	0.20	0.31	0.24	7.4	5.0
5.08	22	0.053	0.40	0.62	0.52	4.8	3.0
5.08	260	0.076	0.40	0.62	0.51	6.6	4.3
10.16	22	0.037	0.80	1.24	0.94	3.6	2.5
10.16	260	0.058	0.80	1.24	1.02	5.1	3.1

[a] Impactor thickness, $h_p = \frac{1}{2}h_t$.
[b] At spall plane.

dependent on V_I and on target thickness. Taylor indicated there may be a relation between this behavior and twinning in copper. Since twinning can be an important mode of deformation in beryllium,[19] this departure from "expected" behavior may be partially due to the operation of twinning as a loss mechanism. A photomicrograph of a recovered specimen from an EOS test is shown in Fig. 10. The beryllium was shocked to 8 kbar at 260°C and extensive twinning is evident (compared with unshocked material in Fig. 3).

Spall Threshold

The incipient spall threshold was determined for elastic pulse widths of nominally 0.2, 0.4, and 0.8 μsec. Results are given in Fig. 11 and Table 1. As mentioned earlier, because of the relatively complicated stress-time history at the spall plane, the pulse widths ΔT_e and ΔT_p and the stress P_I are reference values only. Some calculations were made of the stress-time history at the nominal spall plane using a modification of SWAP-7,[20] a computer code based on the method of characteristics. Typical results are shown in Fig. 12. Table 1 shows that calculated spall plane tensile stress P_s is 30% to 40% less than impact stress, while calculated pulse width ΔT_c was generally about midway between elastic pulse width ΔT_e and plastic pulse width ΔT_p. It is not expected that calculations of the type represented by Fig. 12 would give the actual or exact stress-time history since wave profile measurements show a ramped front with significant rounding of the elastic and plastic waves, which was not taken into account in the calculations. Also, strain rate sensitivity and strain hardening, or possible differences in compressive yielding compared to release yielding, were not considered and these factors will influence material behavior. However, the calculations demonstrate the importance of developing improved spallation criteria for use in computational programs.

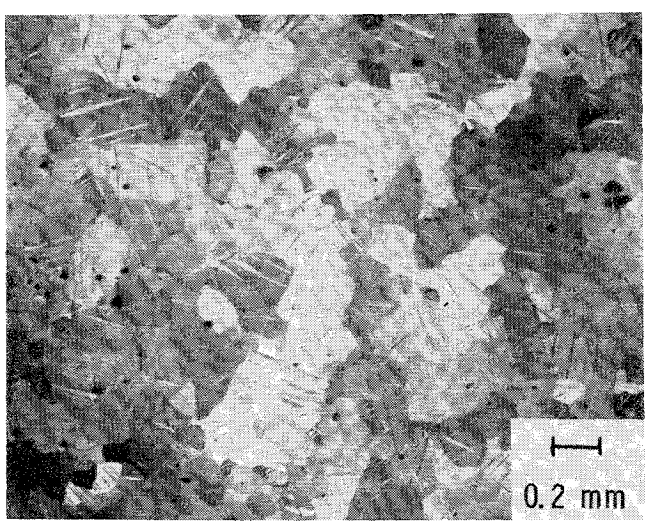

Fig. 10 Beryllium, shocked to 8 kbar (unetched).

Qualitatively, the results in Fig. 11 are similar to those reported for several beryllium alloys (appreciable quantities of BeO): The spall threshold is both time dependent (increasing with decreasing pulse width) and temperature dependent (increasing with temperature change of 22°C to 260°C). Quantitatively, this beryllium has significantly lower threshold velocities than does beryllium with higher BeO content and smaller grains (e.g., N50A,[6] S-200,[7] and I-400[21]). Although there is evidence of a sharply increasing threshold velocity at shorter pulse widths (<0.2 μsec) in other berylliums,[7] the present data justify only a linear fit to the data over the range of pulse widths studied. The "uncertainty" bars in Fig. 11 reflect four factors: 1) effect of data interpolation; 2) velocity measurement error; 3) material scatter; and 4) impactor thickness variation.

A photomicrograph of a typical spall specimen is shown in Fig. 13. Based on the observed spall behavior in this beryllium, some general metallurgical comments can be made.§ Fractures in the incipient or threshold range are transgranular in nature and first appear in a few scattered grains. The microcracks are not confined to the center or nominal spall plane, but spread as velocity increases to cover approximately the center half of the specimen. At high velocities (about twice the threshold velocity) macrocracks (visible to the naked eye) begin to develop at or near the spall plane. The observed transgranular cracking in selected grains at relatively low-impact velocities has probably resulted from the following.[27-32]

1) Because of the limited deformation modes characteristic of hexagonal-close-packed metals such as beryllium, grains oriented with their "weak direction" parallel to the direction of applied tension may be first to exhibit fracture from basal cleavage.

2) Dislocation pile-ups resulting from strain discontinuities at grain boundaries can relax to nucleate cracks.

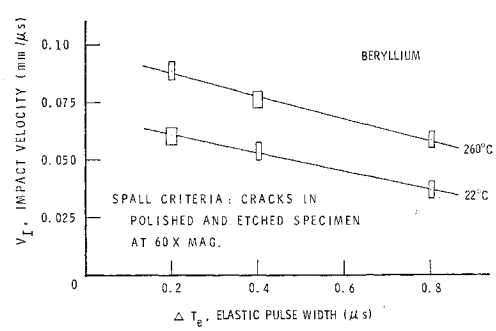

Fig. 11 Spall results.

§ Detailed treatments of the deformation and fracture behavior of beryllium can be found in Refs. 19 and 22–26.

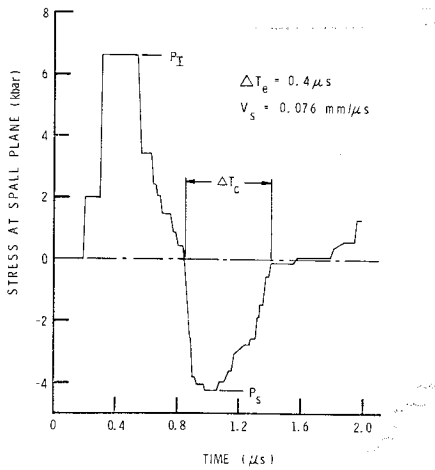

Fig. 12 Stress-time history, spall plane.

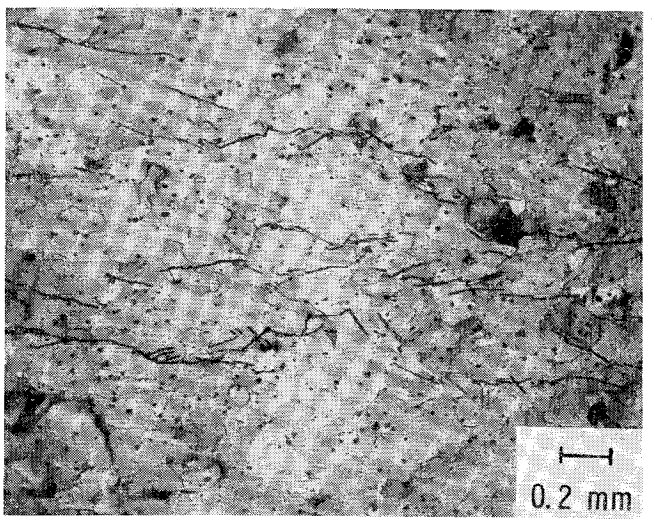

Fig. 13 Beryllium, spalled, 5.08-mm target impacted at 0.090 mm/μsec and 22°C (etched).

3) The relatively large grain size may partially account for the low-spallation threshold (compared to other berylliums) since both yield and fracture strength of beryllium have been found to decrease with increasing grain size.

The increase in threshold velocity for a temperature increase of 22°C to 260°C may be related to the brittle-ductile transition which occurs in beryllium. This transition is characterized by an increase in ductility as temperature increases in the region of the transition temperature, T_c. Although often cited as a specific temperature, T_c is actually a range in temperature over which ductility, generally in terms of tensile elongation-to-fracture, shows a large increase. This temperature is dependent on the following factors:[29,31,33] 1) material composition, i.e., impurity or alloy content, with T_c increasing with impurity content; 2) fabrication history, primarily in terms of texture, anisotropy and grain size, with T_c increasing with grain size; and 3) strain rate, with T_c increasing with strain rate.

T_c has not been directly determined for this beryllium, but is probably in the range of 200 to 300°C.[31] The transition to ductile behavior should coincide with a transition in the fracture mode from transgranular to intergranular.[34] Since the spall photomicrographs still show a predominantly cleavage type fracture, it appears that the material is still in the transition region at 260°C and higher temperature should result in a further increase in ductility and spall threshold.

Although hardness of this beryllium was not measured at 260°C, measurements were made on test specimens before and after heating at 260°C for 10 min. No measurable change in hardness as the result of either heating or impacting was observed. The average hardness was 48 R_A (60-kg load, diamond cone penetrator).

Summary

The Hugoniot equation of state of the subject beryllium for pressures of 3 to 50 kbars can be expressed as

$$P = 0.8 + 149u_p + 32u_p^2$$

This applies to material temperature of 22°C to 260°C. There is a transition region between the preceding EOS and the elastic Hugoniot, $\rho_0 C_L = 236$ kbar/mm/μsec. This region is evidenced by a ramped transition from the dispersive elastic precursor to the plastic wave. Rear free-surface velocity for like-material impacts was found to be about 10% less than impact velocity.

The incipient spall threshold of the subject beryllium, expressed in terms of the impact velocity required for the onset of fracture, increases with decreasing tensile pulse width or time of loading, and increases with increasing material temperature (22°C to 260°C). The spall threshold is significantly lower than that reported for other berylliums,[6,7,21] probably due to differences in impurity content, grain size, and fabrication history.

References

[1] Skidmore, I. C., "An Introduction to Shock Waves in Solids," *Applied Materials Research*, Vol. 4, July 1965, pp. 131–147; also see Al'tshuler, L. V., "Use of Shock Waves in High-Pressure Physics," *Soviet Physics Uspekhi*, Vol. 8, No. 1, July-Aug. 1965, pp. 52–91; Zukas, E. G., "Shock-Wave Strengthening," *Metals Engineering Quarterly*, Vol. 6, May 1966, pp. 1–20; and Oscarson, J. H. and Graff, K. F., "Spall Fracture and Dynamic Response of Materials," Summary Report, BAT-197A-4-3, 1968, Battelle Memorial Institute, Columbus, Ohio.

[2] Christman, D. R., Froula, N. H., and Babcock, S. G., "Dynamic Properties of Three Materials, Volume I: Beryllium," Final Report, MSL-68-33, Nov. 1968, General Motors Manufacturing Development, Warren, Mich.

[3] Butcher, B. M. et al., "Influence of Stress History on Time-Dependent Spalls in Metals," *AIAA Journal*, Vol. 2, No. 6, June 1964, pp. 977–990.

[4] Thurston, R. S. and Mudd, W. L., "Spallation Criteria for Numerical Calculations," LA-4013, Sept. 1968, Los Alamos Scientific Lab., N. Mex.

[5] Tuler, F. R. and Butcher, B. M., "A Criterion for the Time Dependence of Dynamic Fracture," *International Journal of Fracture Mechanics*, Vol. 4, Dec. 1968, pp. 431–437.

[6] Warnica, R. L., "Spallation Thresholds of N50A Beryllium," Final Report, MSL-68-1, Feb. 1968, General Motors Manufacturing Development, Warren, Mich.

[7] Warnica, R. L., "Spallation Thresholds of S-200 Beryllium, ATJ-S Graphite and Isotropic Boron Nitride at 72°F and 1000°F," Final Report, MSL-68-18, July 1968, General Motors Manufacturing Development, Warren, Mich.

[8] Karnes, C. H., "The Plate Impact Configuration for Determining Mechanical Properties of Materials at High Strain Rates," *Mechanical Behavior of Materials under Dynamic Loads*, Springer-Verlag, New York, 1968, pp. 270–293.

[9] Graham, R. A., Neilson, F. W., and Benedick, W. B., "Piezoelectric Current from Shock-Loaded Quartz-A Submicrosecond Stress Gauge," *Journal of Applied Physics*, Vol. 36, May 1965, pp. 1775–1783.

[10] Barker, L. M. and Hollenbach, R. E., "System for Measuring Dynamic Properties of Materials," *Review of Scientific Instruments*, Vol. 35, No. 6, June 1964, pp. 742–746.

[11] Barker, L. M., "Fine Structure of Compressive and Release Wave Shapes in Aluminum Measured by the Velocity Interferometer Technique," *Behavior of Dense Media Under High Dynamic Pressures*, Gordon and Breach, New York, 1968, pp. 483–505.

[12] Smith, J. H., "Three Low-Pressure Spall Thresholds in Copper," *Dynamic Behavior of Materials*, American Society for Testing Materials, Philadelphia, Pa., 1963, pp. 264–282.

[13] Frankeny, J. L. and Floyd, D. R., "Ingot-Sheet Beryllium Fabrication," RFP-910, Feb. 1968, Dow Chemical Co., Rocky Flats Div., Golden, Colo.

[14] Beitscher, S., "Tensile Properties of Rocky Flats Division Ingot-Sheet Beryllium from Room Temperature to 250°C," RFP-1205, Dec. 1968, Dow Chemical Co., Rocky Flats Div., Golden, Colo.

[15] McQueen, R. G. and Marsh, S. P., GMX-6-566, 1964, Los Alamos Scientific Lab., N. Mex., pp. 51–62; also in *Compendium of Shock Wave Data*, UCRL-50108, Secs. A-1, A-2, edited by M. Van Theil, Vol. 1, June 1966.

[16] Munson, D. E., "Dynamic Behavior of Beryllium," SC-RR-67-368, June 1967, Sandia Corp., Albuquerque, N. Mex.

[17] Taylor, J. W., "Stress Wave Profiles in Several Metals," *Dislocation Dynamics*, McGraw-Hill, New York, 1968, pp. 573–589.

[18] Froula, N. H., "The Hugoniot Equation of State of S-200 Beryllium to 1000°F," Final Report, MSL-68-16, July 1968, General Motors Manufacturing Development, Warren, Mich.

[19] Conrad, H. and Perlmutter, I., "Beryllium as a Technological Material," AFML-TR-65-310, Nov. 1965, Air Force Materials Lab., Wright-Patterson Air Force Base, Ohio.

[20] Barker, L. M., "SWAP-7: A Stress-Wave Analyzing Program," SC-RR-67-143, April 1967, Sandia Corp., Albuquerque, N. Mex.

[21] Charest, J. A. and Warnica, R. L., "Spallation Thresholds of I-400 Beryllium," Final Report, TR-66-34, July 1966, General Motors Defense Research Lab., Goleta, Calif.

[22] *The Metal Beryllium*, edited by D. W. White and J. E. Burke, American Society for Metals, Metals Park, Ohio, 1955.

[23] *The Metallurgy of Beryllium*, Chapman and Hall, Ltd., London, England, 1963.

[24] *Beryllium Technology*, Vol. 1, AIME Metallurgical Society Conferences, Gordon and Breach, New York, 1966.

[25] Conrad, H., Blades, J., and Lalevic, B., "Critical Evaluation of the Mechanical Behavior of Beryllium," AFML-TR-66-332, Oct. 1966, Air Force Materials Lab., Wright-Patterson Air Force Base, Ohio.

[26] Hanes, H. D. et al, "Physical Metallurgy of Beryllium," DMIC Rept. 230, June 1966, Battelle Memorial Institute, Columbus, Ohio.

[27] Stroh, A. N., "The Cleavage of Metal Single Crystals," *Philosophical Magazine*, Vol. 3, May 1958, pp. 597–606.

[28] Moore, A. and Lord, W. B. H., "The Development of Beryllium for Use in Aircraft," *Metals for the Space Age: Plansee Proceedings 1964*, Metallwork Plansee AG., Reutte/Tyrol, 1965, pp. 588–612.

[29] Stroh, A. N., "A Theory of the Fracture of Metals," *Advances in Physics*, Vol. 6, 1957, pp. 418–465.

[30] Thevenow, V. H., Herman, M., and Betner, D. R., "Mechanisms of Crack Initiation in Wrought Polycrystalline Beryllium," AFML-TR-68-173, June 1968, Air Force Materials Lab., Wright-Patterson Air Force Base, Ohio.

[31] Armstrong, R. W., "Theory of the Tensile Ductile-Brittle Behavior of Polycrystalline H. C. P. Materials with Application to Beryllium," *Acta Metallurgica*, Vol. 16, March 1968, pp. 347–355.

[32] Bunshah, R. F. and Armstrong, R. W., "The Dependence of the Hardness of Beryllium on Grain Size," *Materials Research Bulletin*, Vol. 4, April 1969, pp. 239–250.

[33] Jacobsen, M. I., "Factors Affecting the Ductile-Brittle Transition in Beryllium," *Beryllium Technology*, Vol. 1, Gordon and Breach, New York, 1966, pp. 249–291; also ASD-TDR-62-509, Vol. V, July 1964, Air Force Materials Lab., Wright-Patterson Air Force Base, Ohio.

[34] Martin, A. J. and Ellis, G. C., "The Ductility Problem in Beryllium," *The Metallurgy of Beryllium*, Chapman and Hall, London, England, 1963, pp. 3–32.